

Vibration of low amplitude imaged in amplitude and phase by sideband versus carrier correlation digital holography

N. Verrier^{1,2}, L. Alloul¹ and M. Gross¹

¹Laboratoire Charles Coulomb - UMR 5221 CNRS-UM2 Université Montpellier II Bat 11. Place Eugène Bataillon 34095 Montpellier

²Laboratoire Hubert Curien UMR 5516 CNRS-Université Jean Monnet 18 Rue du Professeur Benoît Lauras 42000 Saint-Etienne

Sideband holography can be used to get fields images (E_0 and E_1) of a vibrating object for both the carrier (E_0) and the sideband (E_1) frequency with respect to vibration. We propose here to record E_0 and E_1 sequentially, and to image the correlation $E_1 E_0^*$. We show that this correlation is insensitive the phase related to the object roughness and directly reflect the phase of the mechanical motion. The signal to noise can be improved by averaging the correlation over neighbor pixel. Experimental validation is made with vibrating cube of wood and with a clarinet reed. At 2 kHz, vibrations of amplitude down to 0.01 nm are detected.

PACS numbers: 120.7280,090.1995,040.2840,120.2880

Citation: N. Verrier, L. Alloul, and M. Gross, Opt. Lett. 40, 411-414 (2015)
<http://dx.doi.org/10.1364/OL.40.000411>

There is a big demand for full field vibration measurements, in particular in industry. Different holographic techniques are able to image and analyze such vibrations. Double pulse [1, 2] or multi pulse holography [3] records several holograms with time separation in the 1...1000 μ s range, getting the instantaneous velocity from the phase difference. If the vibration frequency is not too high, one can also directly track the vibration of the object with fast CMOS cameras [4, 5]. The analysis of the motion can be done by phase difference or by Fourier analysis in the time domain. For periodic vibration motions, measurements can be done with slow camera. Indeed, an harmonically vibrating object illuminated by a laser yields alternate dark and bright fringes [6], that can be analyzed by time averaged holography [7]. Although the time averaged method gives a way to determine the amplitude of vibration [8] quantitative measurement remains quite difficult for low and high vibration amplitudes.

We have developed heterodyne holography [9, 10], which is a variant of phase shifting holography, in which the frequency, phase and amplitude of both reference and signal beam are controlled by acousto optic modulators (AOM). Heterodyne holography is thus extremely versatile. By shifting the frequency of the local oscillator ω_{LO} with respect to illumination ω_0 , it is for example possible to detect the holographic signal at a frequency ω different than illumination ω_0 . This ability is extremely useful to analyze vibration, since heterodyne holography can detect selectively the signal that is scattered by object on vibration sideband of frequency $\omega_m = \omega_0 + m\omega_A$, where ω_A is the vibration frequency and m and integer index.

As was reported by Ueda et al, [11] the detection of the sideband $m=1$ is advantageous when the vibration amplitude is small. Nanometric vibration amplitude measurements were achieved with sideband digital holography on the $m = 1$ sideband [12], and comparison with single point laser interferometry has been made [13]. Verrier et

al. [14] have shown that one can simultaneously measure E_0 and E_1 by using a local oscillator with two frequency components. One can thus infer the mechanical phase of the vibration [15]. However, Bruno et al [16] shows that this simultaneous detection of E_0 and E_1 can lead to cross talk, and to a loss of detection sensitivity, which becomes annoying when the vibration amplitude is small.

In this letter, we show that simultaneous detection of E_0 and E_1 is not necessary, and that equivalent or superior performances can be obtained by detecting E_0 and E_1 sequentially. Indeed, the cross talk effects seen by Bruno et al. [16] disappear in that case. We also show that the random phase variations caused by the roughness of the object can be eliminated by calculating the correlation $E_1 E_0^*$. It is then possible to increase the signal to noise ratio (SNR) by averaging correlation over neighboring pixels. The sequential measurement of E_0 and E_1 , and the calculation of the correlation $E_1 E_0^*$, make possible to image the vibration “full field”, and to measure quantitatively its amplitude and phase. Maximum sensitivity is achieved by focusing the illumination in the studied point and by averaging the correlation in that region. Finally, we prove that the sensitivity is limited by a sideband signal of one photo-electron per demodulated image sequence. The device and method were validated experimentally by studying a cube of wood vibrating at $\simeq 20$ kHz, and a clarinet reed at $\simeq 2$ kHz. Measurement sensitivity of 0.01 nm for a vibration at 2 kHz, comparable to the sensitivity obtained by Bruno et al. [16] at 40 kHz, is demonstrated.

Consider an object illuminated by a laser at frequency ω_0 that vibrate at frequency ω_A with an out of plane vibration amplitude z_{max} . The out of plane coordinate is $z(t) = z_{max} \sin(\omega_A t)$. The field scattered by the object is $\mathcal{E} = E(t) e^{i\omega_0 t} + c.c.$, where c.c. is the complex conjugate and $E(t)$ the field complex amplitude. In reflection geometry, we have

$$E(t) = E_{wo} e^{i\Phi} \sin(\omega_A t + \arg \Phi)$$

where E_{wo} is the complex field without movement,

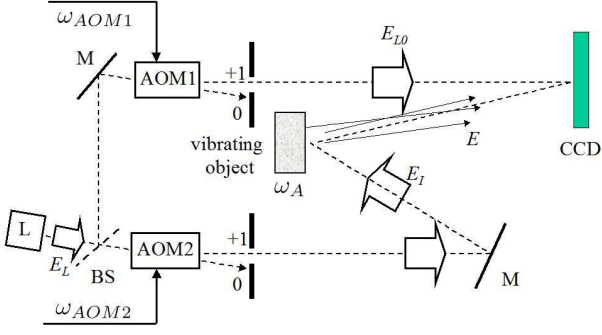


FIG. 1. Heterodyne holography setup applied to analyse vibration. L: main laser; AOM1, AOM2: acousto-optic modulators; M: mirror; BS: beam splitter; CCD: camera.

and Φ is a complex quantity that describes the phase modulation. The phase of this modulation is $\arg \Phi$, while the amplitude is $|\Phi| = 4\pi z_{max}/\lambda$. Because of the Jacobi-Anger expansion, we have $E(t) = E_{wo} \sum_m J_m(|\Phi|) e^{jm(\omega_A t + \arg \Phi)}$ where J_m is the m th-order Bessel function of the first kind. The scattered field \mathcal{E} is then the sum of fields components $\mathcal{E}_m = E_m e^{i\omega_m t} + \text{c.c.}$ of frequency $\omega_m = \omega_0 + m\omega_A$, where m is the sideband index ($m = 0$ for the carrier) with $E_m = E_{wo} J_m(|\Phi|) e^{jm \arg \Phi}$. When the vibration amplitude Φ becomes small, the energy within sidebands decrease very rapidly with the sideband indexes m , and one has only to consider the carrier $m = 0$, and the first sideband $m = \pm 1$. We have thus:

$$\begin{aligned} E_0(\Phi) &= E_{wo} J_0(|\Phi|) \\ E_1(\Phi) &= E_{wo} J_1(|\Phi|) e^{j \arg \Phi} \end{aligned} \quad (1)$$

Note that time averaged holography [7] that detects the carrier field E_0 is not efficient in detecting small amplitude vibration $|\Phi|$, because E_0 varies quadratically with $|\Phi|$. On the other hand, sideband holography that is able to detect selectively the sideband field E_1 is much more sensitive, because E_1 varies with linearly with $|\Phi|$.

One must notice that the field scattered by the sample without vibration E_{wo} depends strongly on the x, y position. In a typical experiment, the sample rugosity is such that this field is a fully developed speckle. The reconstructed fields E_0 and E_1 are thus random in phase, from one pixel (x, y) to the next $(x + 1, y)$. One cannot thus simply extract the phase of the vibration from a measurement made on a single sideband. To remove the pixel to pixel random phase of E_{wo} , we propose to record the hologram successively on the carrier $m = 0$ and the sideband $m = 1$, to reconstruct the corresponding field image of the object $E_0(x, y)$ and $E_1(x, y)$, and to calculate and image the correlation $E_1 E_0^*$, since this correlation do not involves E_{wo} , but $|E_{wo}|^2$, which is real and has no phase. Indeed, we have:

$$E_1 E_0^* = |E_{wo}|^2 J_1(|\Phi|) J_0(|\Phi|) e^{j \arg \Phi} \quad (2)$$

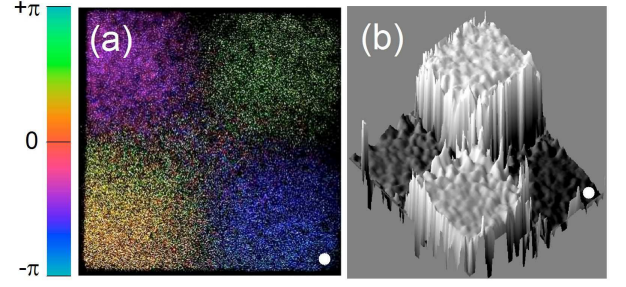


FIG. 2. (a,b) Reconstructed images of a cube of wood vibrating at $\omega_A/2\pi = 21.43$ kHz. (a) $E_1 E_0^*$ correlation image: brightness is amplitude (i.e. $|E_1 E_0^*|$), color is phase (i.e. $\arg E_1 E_0^*$). (b) 3D display of the phase $\arg E_1 E_0^*$.

For small vibration amplitude ($|\Phi| \ll 1$), correlation simplifies to $E_1 E_0^* \simeq |E_{wo}|^2 \Phi/2$. Correlation $E_1 E_0^*$ is a powerful tool since gives directly the phase of mechanical motion $\arg \Phi$. Nevertheless, problems can be encountered when the signal $|E_{wo}|^2$ scattered without vibration vanish.

Figure 1 shows the holographic experimental setup used to measure successively E_0 and E_1 in order to get $E_1 E_0^*$. The main laser L is a Sanyo DL-7140-201 diode laser ($\lambda = 785$ nm, 50 mW). It is split into an illumination beam (frequency ω_I , complex field E_I), and in a LO beam (ω_{LO} , E_{LO}). The illumination light scattered by the object interferes with the reference beam on the camera (Lumenera 2-2: 1616×1216 pixels of $4.4 \times 4.4 \mu\text{m}$) whose frame rate is $\omega_{CCD} = 10$ Hz. To simplify further Fourier transform calculations, the 1616×1216 measured matrix is truncated to 1024×1024 .

The illumination and LO beam frequencies ω_{LO} and ω_I are tuned by using two acousto-optic modulators AOM1 and AOM2 (Bragg cells), and we have $\omega_{LO} = \omega_L + \omega_{AOM1}$ and $\omega_I = \omega_L + \omega_{AOM2}$, where $\omega_{AOM1/2} \simeq 80$ MHz are the frequencies of RF signals that drive the AOMs. The RF signals are tuned to have $\omega_{LO} - \omega_I = \omega_{CCD}/4$ to get E_0 , and to have $\omega_{LO} - \omega_I = \omega_A + \omega_{CCD}/4$ to get E_1 . Successive sequences of $n_{max} = 128$ camera frames (i.e. $I_0, I_1 \dots I_{127}$) are recorded by tuning the RF signals first on the carrier (E_0), then on the sideband (E_1). The carrier and sideband complex hologram H are obtained from these sequences by 4 phase demodulation with n_{max} frames:

$$H(x, y) = \sum_{n=0}^{n=n_{max}-1} j^n I_n(x, y) \quad (3)$$

The fields images of the object $E_0(x, y)$ and $E_1(x, y)$ are then reconstructed from H by the Schnars et. al [17] method that involves 1 Fourier transformation. The correlation $E_1 E_0^*$ is then calculated.

Figure 2 (a) shows the reconstructed correlation images of a cube of wood ($2 \text{ cm} \times 2 \text{ cm}$) vibrating at its resonance frequency $\omega_A/2\pi = 21.43$ kHz. Brightness is the

correlation amplitude (i.e. $|E_1 E_0^*|$) and color the correlation phase (i.e. $\arg E_1 E_0^*$). As seen, neighbor point have the same phase (same color). In order to get better SNR for the phase, the complex correlation signal $E_1 E_0^*$ is averaged over neighbor x, y points by using a 2D Gaussian blur filter of radius 4 pixels. Figure 2 (b) displays the phase of the averaged correlation $E_1 E_0^*$ in 3D. As seen, the opposite corners (upper left and bottom right for example) vibrate in phase, while the neighbor corners (upper left and upper right for example) vibrate in phase opposition. Note that the cube is excited in one of its corner by a needle. This may explain why the opposite corners are not perfectly in phase in Fig. 2 (c).

We can go further and use E_0 and E_1 to calculate the vibration complex amplitude Φ . To increase the SNR let us average, over neighbor reconstructed pixels, the correlation $E_1 E_0^*$ and the carrier intensity $|E_0|^2$:

$$|E_0|^2 = |E_{wo}|^2 J_0^2(\Phi) \simeq |E_{wo}|^2 \Phi / 2 \quad (4)$$

By averaging we get:

$$\begin{aligned} \langle E_1 E_0^* \rangle_{x,y} &= (1/N_{pix}) \sum_{x',y'} E_1(x',y') E_0^*(x',y') \quad (5) \\ &\simeq (\Phi(x,y)/2) (1/N_{pix}) \sum_{x',y'} |E_{wo}(x',y')|^2 \\ \langle |E_0|^2 \rangle_{x,y} &\simeq (1/N_{pix}) \sum_{x',y'} |E_{wo}(x',y')|^2 \end{aligned}$$

where $\sum_{x',y'}$ is the summation over the N_{pix} pixels of the averaging zone located around the point of coordinate x, y . The vibration amplitude Φ is then

$$\Phi(x,y) = 2 \langle E_1 E_0^* \rangle_{x,y} / \langle |E_0|^2 \rangle_{x,y} \quad (6)$$

We get here Φ that gives both the amplitude $z_{max} = \lambda |\Phi| / 4\pi$ and the phase $\arg \Phi$ of the mechanical motion. Note that it is also possible to get Φ by calculating the ratio $E_1/E_0 \simeq \Phi$ as done by Verrier et. al [14], but the ratio calculation is unstable for the points x, y of the object where E_{wo} is close to zero.

To evaluate the limits of sensibility of the correlation + averaging method, we have calculated by Monte Carlo the detection limit of $|\Phi|$, for an ideal holographic detection that is only limited by shot noise. The calculation is similar to one made by Lesaffre et al. [18]. For each pixel (x, y) , each frame (n) and each sequence ($m=0$ or $m=1$), we have calculated the ideal camera signal I'_n in the absence of shot noise. We have $I'_n = |E_{LO} + j^n E'_{0/1}|^2$, where the factor j^n accounts for the phase shift of the local oscillator field E_{LO} with respect to object field $E_{0/1}$ for frame n . To account for the roughness of the sample, E'_0 and E'_1 are taken proportional to a Gaussian speckle $E'_{wo}(x, y)$ that is uncorrelated from one pixel to the next, but remains the same for all frames n and all sequences $m=0$ or 1 . To account for shot noise, we have added to I'_n a Gaussian random noise s of variance of $\sqrt{I'_n}$, where I'_n is expressed in electron photo electron Units. The noise s is uncorrelated from one pixels x, y to another, from

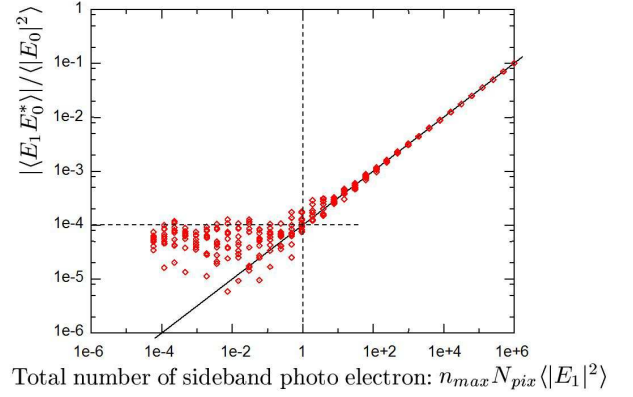


FIG. 3. Ratio $|\langle E_1 E_0^* \rangle| / \langle |E_0|^2 \rangle$ calculated by Monte Carlo by decreasing the sideband signal $|E_1|^2$. Horizontal axis is the total sideband energy: $n_{max} N_{pix} \langle |E_1|^2 \rangle$ in photo electron Units. Simulation is made with $n_{max}=400$, $N_{pix} = 50^2$, $|E_{LO}|^2 = 10^4$ and $|E_0|^2 = 10^2$ photo electrons.

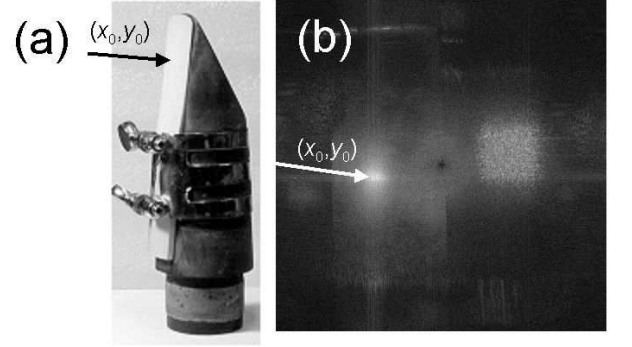


FIG. 4. (a) Clarinet reed with illumination beam focused in x_0, y_0 . (b) Sideband $m = 1$ reconstructed image of the vibrating reed. The display is made in arbitrary log scale for the field intensity $|E_1(x, y)|^2$.

one frame n to another, and from one sequence m to another. By this way, we have obtained the Monte Carlo frame signals $I_n = I'_n + s$ with whom we have performed the 4 phase demodulation with n_{max} frames of Eq. (3). We have then calculated the reconstructed signal E_0 and E_1 , the correlations and intensities $E_1 E_0^*$ and $|E_0|^2$, and the means $\langle E_1 E_0^* \rangle$ and $\langle |E_0|^2 \rangle$. We have then calculated the ratio $\langle E_1 E_0^* \rangle / \langle |E_0|^2 \rangle$ that gives Φ using Eq. (6).

Figure 3 gives the result of the Monte Carlo simulation for the ratio $|\langle E_1 E_0^* \rangle| / \langle |E_0|^2 \rangle$. Each point correspond to simulation made with a double sequence $m=0$ and 1 . The simulation is performed by decreasing the sideband averaged signal field intensity $\langle |E_1|^2 \rangle = 1, 0.5, 0.25 \dots$ photo electron per pixel and per frame. The other parameters of the simulation are $n_{max} = 400$, $N_{pix} = 50^2$, $|E_{LO}|^2 = 10^4$ and $\langle |E_0|^2 \rangle = 10^2$ photo electrons. For each value of $\langle |E_1|^2 \rangle$, 10 simulations are performed. As can be seen in Fig. 3 the ratio $|\langle E_1 E_0^* \rangle| / \langle |E_0|^2 \rangle$ decreases with

the sideband signal E_1 proportionally with $\sqrt{\langle |E_1|^2 \rangle}$. When E_1 becomes very small, the ratio reaches a noise floor related to shot noise. To simplify the present discussion, the results are displayed as a function of the total number of photoelectrons on the sideband $m=1$. The x-axis is thus $n_{max}N_{pix}\langle |E_1|^2 \rangle$. As seen in Fig.3 the noise floor is reached for $n_{max}N_{pix}\langle |E_1|^2 \rangle = 1$. We have verified by making simulation not displayed on Fig.3 that this result does not depend on $|E_{LO}|^2$ and $\langle |E_0|^2 \rangle$, provided that $|E_{LO}|^2 \gg \langle |E_0|^2 \rangle \gg \langle |E_1|^2 \rangle$. The noise floor corresponds thus to a minimal ratio $|\langle E_1 E_0^* \rangle|/\langle |E_0|^2 \rangle = 1/\sqrt{n_{max}N_{pix}\langle |E_0|^2 \rangle}$ (i.e. to 10^{-4}), and to a minimal detectable vibration amplitude $\Phi = 2/\sqrt{n_{max}N_{pix}\langle |E_0|^2 \rangle}$ (i.e. to $2 \cdot 10^{-4}$).

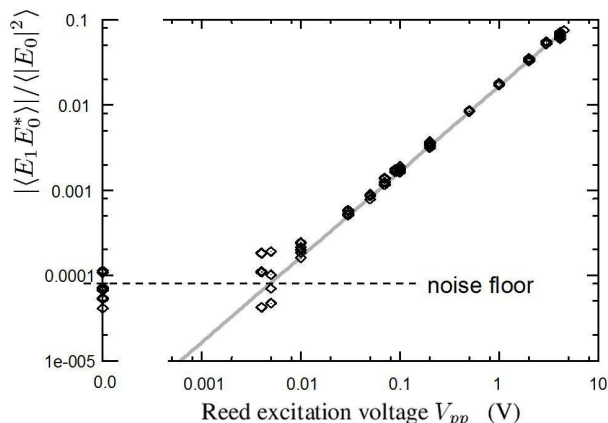


FIG. 5. Ratio $|\langle E_1 E_0^* \rangle|/\langle |E_0|^2 \rangle$ as function of the reed excitation voltage converted in vibration amplitude z_{max} in nm Units. Measurements: dark grey points, and theory $J_1(|\Phi|)/J_0(|\Phi|) \simeq |\Phi|/2$: light grey curve.

We have tested the ability of the correlation + averaging method to measure low vibration amplitude in an experiment made with a vibrating clarinet reed excited at $\omega_A=2$ kHz with a loudspeaker. In order to in-

crease the sensitivity, the vibration amplitude is measured on a single point (x_0, y_0) (see Fig.4 (a)). The illumination has been focused on that point, and the calculations have been made with an averaging region centered on that point, whose size (radius 50 pixels for example) has been chosen to include the whole illumination zone. We have reconstructed the field image of the reed at the carrier frequency (i.e. $E_0(x, y)$) (see Fig.4 (b)), and verified on the holographic data that most of the energy $|E_0|^2$ is within the averaging zone x_0, y_0 . Sequences of $n_{max} = 128$ frames I_n have been recorded for both carrier (E_0) and sideband (E_1), while the peak to peak voltage V_{pp} of the loudspeaker sinusoidal signal has been decreased. We have then calculated H by Eq. (3), reconstructed the fields images of the reed E_0 and E_1 , and calculated the correlation $E_1 E_0^*$, the intensity $|E_0|^2$, and the means $\langle E_1 E_0^* \rangle$ and $\langle |E_0|^2 \rangle$. We have then calculated the ratio $|\langle E_1 E_0^* \rangle|/\langle |E_0|^2 \rangle$. The latter is plotted on Fig.5 as a function of the loudspeaker voltage V_{pp} that is proportional to vibration amplitude Φ . The measured points follow $|\langle E_1 E_0^* \rangle|/\langle |E_0|^2 \rangle \simeq |\Phi|/2 \propto V_{pp}$ down to a vibration amplitude noise floor of $|\Phi| \simeq 7 \cdot 10^{-5}$ that corresponds to $z_{max} \simeq 10^{-2}$ nm i.e. $\lambda/78000$. Note that the noise floor measure here is about $\times 20$ lower than in previous holographic experiments [12, 14] and lower than the limit $\lambda/3500$ predicted by Ueda [11]. Similar noise floor has been detected by holography by Bruno et al. [16], but at much higher vibration frequency (40 kHz).

In future work, it would be interesting to explore the limits of sensitivity of the correlation technique for low vibration amplitude. This can be done by using a laser with lower noise, by increasing the vibration frequency ω_A (and in all case by measuring the laser noise at ω_A). One could also increase the illumination power, and the number of frame of the coherent detection ($n_{max} > 128$). A better control of the vibration ω_A versus camera ω_{CCD} frequencies, and or a proper choice of the demodulation equation could be also important, in order to avoid leak detection of E_0 , when detection is tuned on E_1 .

The Authors wishes to acknowledge ANR-ICLM (ANR-2011-BS04-017-04) for financial support, and M. Lesaffre for fruitful discussion and helpful comments.

-
- [1] G. Pedrini, Y. Zou, and H. Tiziani, "Digital double-pulsed holographic interferometry for vibration analysis," *J. Mod. Opt.* **42**, 367–374 (1995).
 - [2] G. Pedrini, H. J. Tiziani, and Y. Zou, "Digital double pulse-TV-holography," *Opt. Las. Eng.* **26**, 199–219 (1997).
 - [3] G. Pedrini, P. Froening, H. Fessler, and H. Tiziani, "Transient vibration measurements using multi-pulse digital holography," *Opt. Las. Technol.* **29**, 505–511 (1998).
 - [4] G. Pedrini, W. Osten, and M. E. Gusev, "High-speed digital holographic interferometry for vibration measurement," *Appl. Opt.* **45**, 3456–3462 (2006).
 - [5] Y. Fu, G. Pedrini, and W. Osten, "Vibration measurement by temporal Fourier analyses of a digital hologram sequence," *Appl. Opt.* **46**, 5719–5727 (2007).
 - [6] R. L. Powell and K. A. Stetson, "Interferometric vibration analysis by wavefront reconstruction," *J. Opt. Soc. A* **55**, 1593–1597 (1965).
 - [7] P. Picart, J. Leval, D. Mounier, and S. Gougeon, "Time-averaged digital holography," *Opt. Lett.* **28**, 1900–1902 (2003).
 - [8] P. Picart, J. Leval, D. Mounier, and S. Gougeon, "Some opportunities for vibration analysis with time averaging in digital Fresnel holography," *Appl. Opt.* **44**, 337–343 (2005).
 - [9] F. Le Clerc, L. Collot, and M. Gross, "Numerical heterodyne holography with two-dimensional photodetector

- arrays,” *Opt. Lett.* **25**, 716–718 (2000).
- [10] F. Le Clerc, M. Gross, and L. Collot, “Synthetic-aperture experiment in the visible with on-axis digital heterodyne holography,” *Opt. Lett.* **26**, 1550–1552 (2001).
- [11] M. Ueda, S. Miida, and T. Sato, “Signal-to-noise ratio and smallest detectable vibration amplitude in frequency-translated holography: an analysis,” *Appl. Opt.* **15**, 2690–2694 (1976).
- [12] P. Psota, V. Ledl, R. Dolecek, J. Erhart, and V. Kopecky, “Measurement of piezoelectric transformer vibrations by digital holography,” *IEEE T. Ultrason. Ferr.* **59**, 1962–1968 (2012).
- [13] P. Psota, V. Lédl, R. Doleček, J. Václavík, and M. Šulc, “Comparison of digital holographic method for very small amplitudes measurement with single point laser interferometer and laser Doppler vibrometer,” in *Digital Holography and Three-Dimensional Imaging* pp. DSu5B–3 (2012).
- [14] N. Verrier and M. Atlan, “Absolute measurement of small-amplitude vibrations by time-averaged heterodyne holography with a dual local oscillator,” *Opt. Lett.* **38**, 739–741 (2013).
- [15] F. Bruno, J.-B. Laudereau, M. Lesaffre, N. Verrier, and M. Atlan, “Phase-sensitive narrowband heterodyne holography,” *Appl. Opt.* **53**, 1252–1257 (2014).
- [16] F. Bruno, J. Laurent, D. Royer, and M. Atlan, “Holographic imaging of surface acoustic waves,” *Appl. Phys. Lett.* **104**, 083 504 (2014).
- [17] U. Schnars and W. Juptner, “Direct recording of holograms by a CCD target and numerical reconstruction,” *Appl. Opt.* **33**, 179–181 (1994).
- [18] M. Lesaffre, N. Verrier, and M. Gross, “Noise and signal scaling factors in digital holography in weak illumination: relationship with shot noise,” *Appl. Opt.* **52**, A81–A91 (2013).